ELECTRONIC SUPPLEMENTARY INFORMATION

pH response and molecular recognition in a low molecular weight peptide hydrogel

Stefanie C. Lange[a], Jan Unsleber[a], Patrick Drücker[b], Hans-Joachim Galla[b], Mark Waller[a], Bart Jan Ravoo*[a]

Email: b.j.ravoo@uni-muenster.de

TABLE OF CONTENTS

METHODS

All side chain and Fmoc protected amino acids used for SPPS were purchased from NOVABIOCHEM (MERCK BIOSCIENCES AG, Läufelfingen, Switzerland), all other chemicals from SIGMA ALDRICH (Taufkirchen, Germany) or ACROS ORGANICS (Schwerte, Germany) were used without further purification. All solvents were dried according to the conventional methods before use. DMF for SPPS had peptide synthesis grade. All reactions were carried out in oven-dried flasks and were stirred magnetically. Ultrapure water was used in all analytical measurements and for gel preparations.

Preparative HPLC Purification of final compounds was achieved with a KNAUER preparative HPLC system (Berlin) consisting of a KNAUER pump manager *5050*, KNAUER pump *1050*, KNAUER UV-photometer *2550* and a KNAUER dynamic mixing chamber. Separation was carried out using a VARIAN *VariTide RPC* (250 x 21.2 mm i.d., 200 Å pore size, 6.0 µm particle size) semipreparative HPLC column. Samples were injected over a 5 mL loop dissolved under starting conditions, and fractions were collected with an automatic FOXY R1 *Teledyn ISCO*. The software used for controlling HPLC and Foxy was Chromgate® Version 3.3.2. The flowrate was 8 mL min^{-1} and the UV absorption was monitored at 210 nm, 280 nm and 492 nm. Water (100, 0.01% TFA, **A**) and water/acetonitrile (20:80, 0.01% TFA, **B**) were used as the mobile phase with the following gradient:

t/min	**A**/%	**B**/%
0	95	5
5	95	5
50	20	80
60	20	80
65	95	5
78	95	5

Mass spectra of each fraction collected were recorded using a mALDI *Autoflex speed* (BRUKER DALTONICS GMBH, Bremen). Sample preparation was done using a α-Cyano-4-hydroxycinnamic acid matrix in an acidic mixture of water/acetonitrile/TFA (70:30:1). Samples were spotted on a M*TP 384 target plate ground steel BC*, BRUKER DALTONICS GMBH. Spectra were recorded using a *Nd:YAG* laser with a wavelength of 355 nm and a pulse length of 6 ns.

Analytical HPLC Analysis of HPLC fractions containing the product was achieved with a AGILENT analytical HPLC system of the *1100 series* consisting of a AGILENT degasser *G1379A*, AGILENT quat pump *G1311A*, AGILENT WPALS *G1367A*, AGILENT Colcom *G1316A*, AGILENT DAD *G1315B*, AGILENT man. Inj. *G1328B*. Separation was carried out using an AGILENT *Eclipse XDB-C18* (150 x 2.1 mm i.d., 3.5 µm particle size) analytical HPLC column. The software used for controlling HPLC was Linux4ever® *MK5, Rev. B.01.03[204]* AGILENT TECHNLOGIES 2001-2005. The flowrate was 0.4 mL min^{-1} and the UV

absorption was monitored at 210 nm, 280 nm and 492 nm. The injection volume was 10 µL and water (0.05% TFA, **A**) and water/acetonitrile (20:80, 0.05% TFA, **B**) were used as the mobile phase with the following gradient:

t/min	**A**/%	**B**/%
0	95	5
2	95	5
17	20	80
20	20	80
25	95	5
30	95	5

NMR spectra were recorded on the spectrometer AV400 (BRUKER). All measurements were carried out in deuterated solvents and chemical shifts (δ) recorded in parts per million (ppm) relative to the residual solvent protons. MESTRENOVA 8.1 was used for spectra analysis. Notation was done as follows: s = singulett, d = duplet, t = triplet, q = quartet, m = multiplet.

Mass spectra were recorded on a *Micro tof* (BRUKER DALTONICS GMBH) and *Orbi-Trap LTQ-XL* (THERMO SCIENTIFIC) electrospray ionization spectrometers (ESI) using methanol or water as solvent. Determination of products in HPLC fractions was achieved with matrix assisted laser desorption/ionization (MALDI) techniques on a *Autoflex speed* (BRUKER DALTONICS GMBH). Sample preparation was done using an α-Cyano-4-hydroxycinnamic acid matrix in an acidic mixture of water/acetonitrile/TFA (70:30:1). Samples were spotted on a *MTP 384 target plate ground steel BC* (BRUKER DALTONICS GMBH). Spectra were recorded using a *Nd:YAG* laser with a wavelength of 355 nm and a pulse length of 6 ns. Data notation shows the metrology followed by the used solvent in brackets. Calculated and detected masses are recorded separately.

IR spectra were recorded on a 3100 FT-IR (VARIAN) equipped with a MKII Golden Gate Single Reflection ATR unit. For spectra analysis RESOLUTION PRO was used. Notation was done as follows: s = strong, m = medium, w = weak.

Circular dichroism titrations were performed on a *J 815* CD-spectrometer (JASCO). As background water was measured and subtracted from every sample. Quarz glass cuvettes *104F-QS*, 1.00 mm (BRAND) were used. Spectra were recorded between 180 and 300 nm and analyzed with the software *Spectra manager Version 2.08.04* (JASCO). Data analysis was performed using *Origin 8.5 version 8.0724(B724)* (ORIGINLAB COOPERATIONS, Northhampton, USA).

OD600 measurements were performed on a doublestream UV-spectrometer *Uvikon 923* (KONTRON INSTRUMENTS, Zürich (CH) using a constant wavelength of $\lambda = 600$ nm and PMMA cuvettes (BRAND GMBH & CO KG, Wertheim).

AFM experiments employed a NanoWizard® 3 AFM (JPK Instruments AG, Berlin, Germany) on a Zeiss Axio Observer D.1 (Carl Zeiss AG, Oberkochen, Germany). Data analysis was done using GWYDDION, *Version 2.36.* Intermittent contact measurements were done at 1 Hz line rate using *RTESP* cantilever (VEECO) with a nominal spring constant of k = 20-80 N/m, containing a phosphorous doped Si tip with a nominal radius of < 10 nm.

Small-angle X-ray scattering (SAXS) experiments were performed at the European Synchrotron Radiation Facility (ESRF) in Grenoble, France, at the high-brilliance beamline ID02. An X-ray energy of 12.46 keV and sample-to-detector distance of 1.5 m was used to cover a q-range of $0.007 < q < 0.4486$ Å^{-1}, with q being the magnitude of the scattering wave vector. The samples were injected into a glass capillary at a temperature of 20 °C. The scattering data were corrected for background scattering, detector response and primary beam intensity fluctuations. The instrument scattering vector was calibrated using a silver behenate standard. Peak positions were determined by taking the midpoint between the local extremes in the first derivative of the scattering intensities. Data analysis and fitting procedures were carried out with *SasView 2.2.1* using an *Ellipticalcyclinder* form factor as shape model.

Fmoc-L-Cys(Acm)-L-His-L-Cys-OH 1

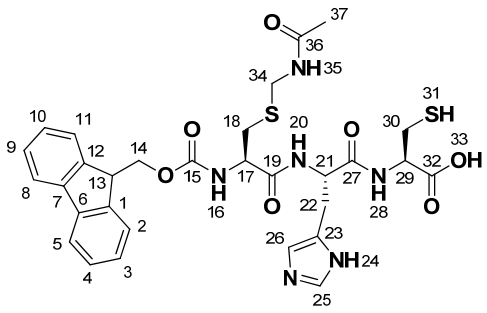

^{1}H NMR (300 MHz, DMSO-d_6, 300 K) δ 13.90 (s, 1H, 33-H), 8.90 (s, 1H, 25-H), 8.60 (t, $^3J_{HH}$ = 6.5 Hz, 1H, 35-H), 8.32 (d, $^3J_{HH}$ = 8.1 Hz, 1H, 28-H), 8.22 (d, $^3J_{HH}$ = 7.8 Hz, 1H, 20-H), 7.89 (d, $^3J_{HH}$ = 7.5 Hz, 2H, 5,8-H), 7.76 – 7.68 (m, 3H, 2,11,16-H), 7.42 (t, $^3J_{HH}$ = 7.4 Hz, 2H, 4,9-H), 7.37 – 7.26 (m, 3H, 3,10,24,26-H), 4.73 – 4-62 (m, 1H, 29-H), 4.49 – 4.39 (m, 1H, 21-H), 4.39 – 4.12 (m, 6H, 13,14,17,34-H), 3.23 – 2.95 (m, 2H, 22-H), 2.95 – 2.60 (m, 4H, 18,30-H), 1.86 (s, 3H, 37-H) ppm.

^{13}C{^{1}H}-NMR (75 MHz, DMSO-d_6, 300 K) δ 171.4 (s, C-32), 170.9 (s, C-36), 170.1 (s, C-19), 169.9 (s, C-27), 156.1 (s, C-15), 143.8 (s, C-1,12), 140.8 (s, C-6,7), 133.8 (s, C-25), 129.2 (s, C-23), 127.7 (s, C-4.9), 127.2 (s, C-3,10), 125.4 (s, C-2,11), 120.2 (s, C-5,8), 117.0 (s, C-26), 65.9 (s, C-14), 54.6 (s, C-17,21), 51.6 (s, C-29), 46.6 (s, C-13), 39.9 (s, C-34), 32.1 (s, C-18), 27.0 (s, C-22), 25.5 (s, C-30), 22.6 (s, C-37) ppm.

ESI$^+$ (MeOH): calc.: m/z = 655.2003 $[M+H]^+$, 677.1823 $[M+Na]^+$; det.: m/z = 655.2029 $[M+H]^+$, 677.1803 $[M+Na]^+$.

IR (ATR): ν = 3287 (m), 3149 (w), 3043 (w), 1644 (s), 1527 (s), 1450 (w), 1426 (w), 1373 (w), 1319 (w), 1235 (w), 1187 (s), 1137 (m), 1091 (w), 1039 (m), 996 (w), 836 (m), 796 (w), 757 (w), 739 (m), 727 (m), 634 (w), 598 (w) cm^{-1}.

Fmoc-L-Cys-L-His-L-Cys-OH 2

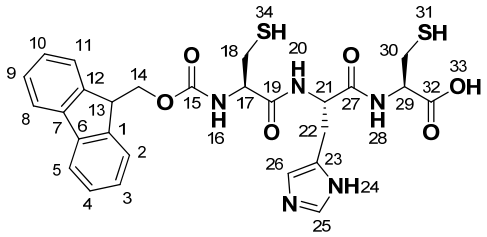

^{1}H NMR (400 MHz, DMSO-d_6, 300 K) δ 13.99 (s, 1H, 33-H), 8.92 (d, $^3J_{HH}$ = 8.5 Hz, 1H, 25-H), 8.49 (d, $^3J_{HH}$ = 8.2 Hz, 1H, 20-H), 8.21 (d, $^3J_{HH}$ = 7.8 Hz, 1H, 28-H), 7.91 – 7.86 (m, 2H, 5,8-H), 7.76 – 7.69 (m, 2H, 2,11-H), 7.66 (d, $^3J_{HH}$ = 8.1 Hz, 1H, 16-H), 7.45 – 7.37 (m, 2H, 4,9-H), 7.36 – 7.29 (m, 3H, 3,10,26-H), 4.71 – 4.62 (m, 1H, 21-H), 4.48 – 4.40 (m, 1H, 29-H), 4.40 – 4.18 (m, 3H, 13,14-H), 4.15 – 4.07 (m, 1H, 17-H), 3.20 – 2.94 (m, 3H, 22,34-H), 3.07 – 2.94 (m, 2H, 18-H$_a$, 30-H), 2.71 – 2.61 (m, 1H, 18-H$_b$), 2.36 (t, $^3J_{HH}$ = 8.6 Hz, 1H, 31-H) ppm.

^{13}C{^{1}H}-NMR (101 MHz, DMSO-d_6, 300 K) δ 171.3 (s, C-32), 170.4 (s, C-19), 169.9 (s, C-27), 156.1 (s, C-15), 143.9 (s, C-1,12), 140.8 (s, C-6,7), 133.7 (s, C-25), 129.3 (s, C-23), 127.7 (s, C-4,9), 127.2 (s, C-3,10), 125.4 (s, C-2,11), 120.2 (s, C-5,8), 117.0 (s, C-26), 65.8 (s, C-14), 57.5 (s, C-17), 54.6 (s, C-29), 51.7 (s, C-21), 46.7 (s, C-13), 26.8 (s, C-22), 26.0 (s, C-18), 25.5 (s, C-30) ppm.

ESI$^+$ (MeOH): calc.: m/z = 584.1632 $[M+H]^+$, 606.1451 $[M+Na]^+$; det.: m/z = 584.1631 $[M+H]^+$, 606.1442 $[M+Na]^+$.

IR (ATR): ν = 3292 (w), 3148 (w), 1645 (s), 1529 (m), 1448 (w), 1425 (w), 1320 (w), 1186 (s), 1138 (s), 1089 (w), 1035 (w), 850 (m), 739 (m), 728 (m), 700 (m) cm^{-1}.

Ad-TEG-en

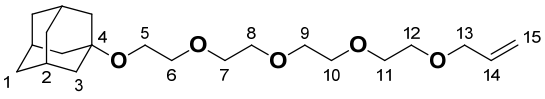

^{1}H-NMR (300 MHz, $CDCl_3$, 300K) δ 5.89 (ddt, $^3J_{HH}$ = 17.2, 10.4, 5.6 Hz, 1H, 14-H), 5.30 - 5.09 (m, 2H, 15-H), 4.00 (dt, $^3J_{HH}$ = 5.7, 1.4 Hz, 2H, 13-H), 3.66 - 3.54 (m, 16H, 5,6,7,8,9,10,11,12-H), 2.11 (br, 3H, 2-H), 1.72 (d, $^3J_{HH}$ = 2.8 Hz, 6H, 3-H), 1.67 - 1.49 (m, 6H, 1-H) ppm.

^{13}C{^{1}H}-NMR (75 MHz, $CDCl_3$, 300 K) δ 134.9 (s, C-14), 117.2 (s, C-15), 72.3 (s, C-4), 72.3 – 59.5 (8s, C-6,7,8,9,10,11,12, 13), 59.3 (s, C-5), 41.5 (s, C-3), 36.5 (s, C-1), 30.6 (s, C-2) ppm.

ESI$^+$ (MeOH): calc.: m/z = 386.2901 $[M+H]^+$, 391.2455 $[M+Na]^+$; det.: m/z = 386.2907 $[M+H]^+$, 391.2484 $[M+Na]^+$.

IR (ATR): ν = 2905 (s), 2852 (s), 1739 (w), 1453 (w), 1354 (w), 1305 (w), 1244 (w), 1106 (s), 1090 (s), 1045 (w), 981 (m), 924 (m), 872 (w) cm^{-1}.

NMR SPECTRA

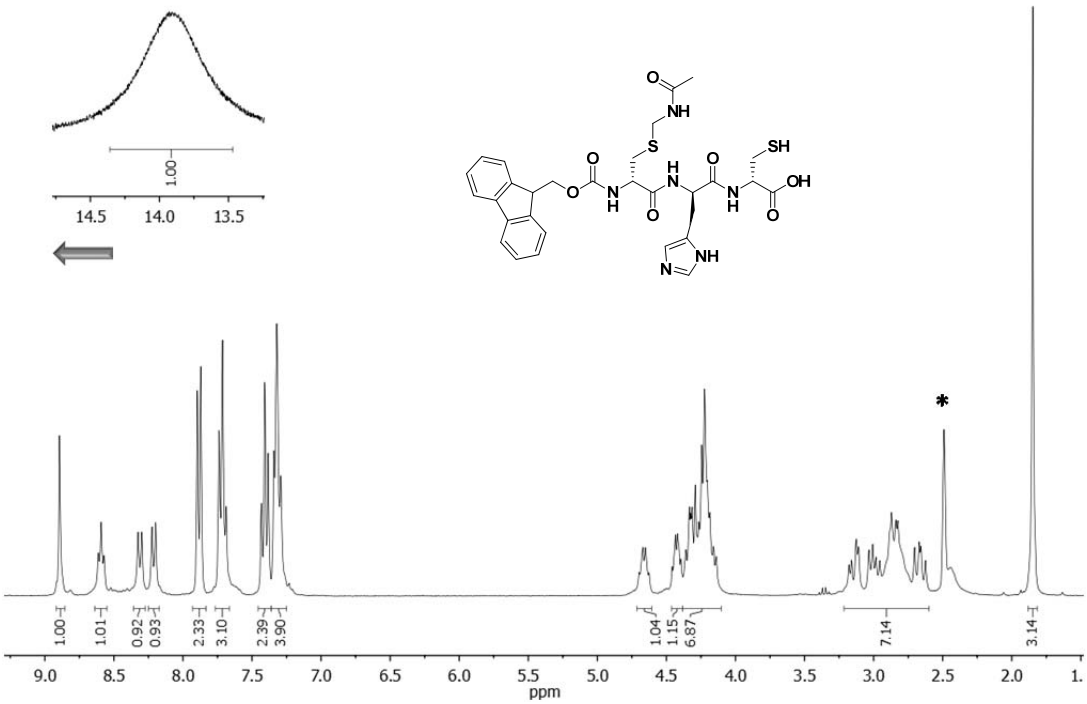

Figure S1: [1]H-NMR spectrum of Fmoc-L-Cys(Acm)-L-His-L-Cys-OH **1** in DMSO-d_6* at 300 K.

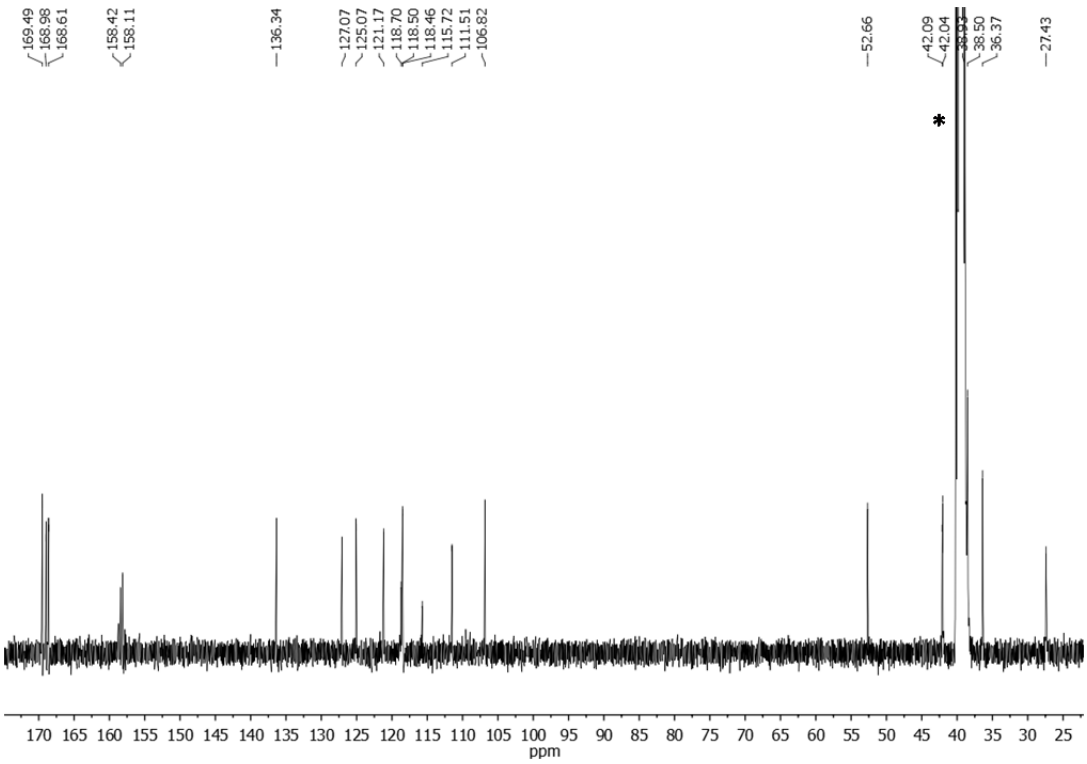

Figure S2: [13]C-NMR spectrum of Fmoc-L-Cys(Acm)-L-His-L-Cys-OH **1** in DMSO-d_6* at 300 K.

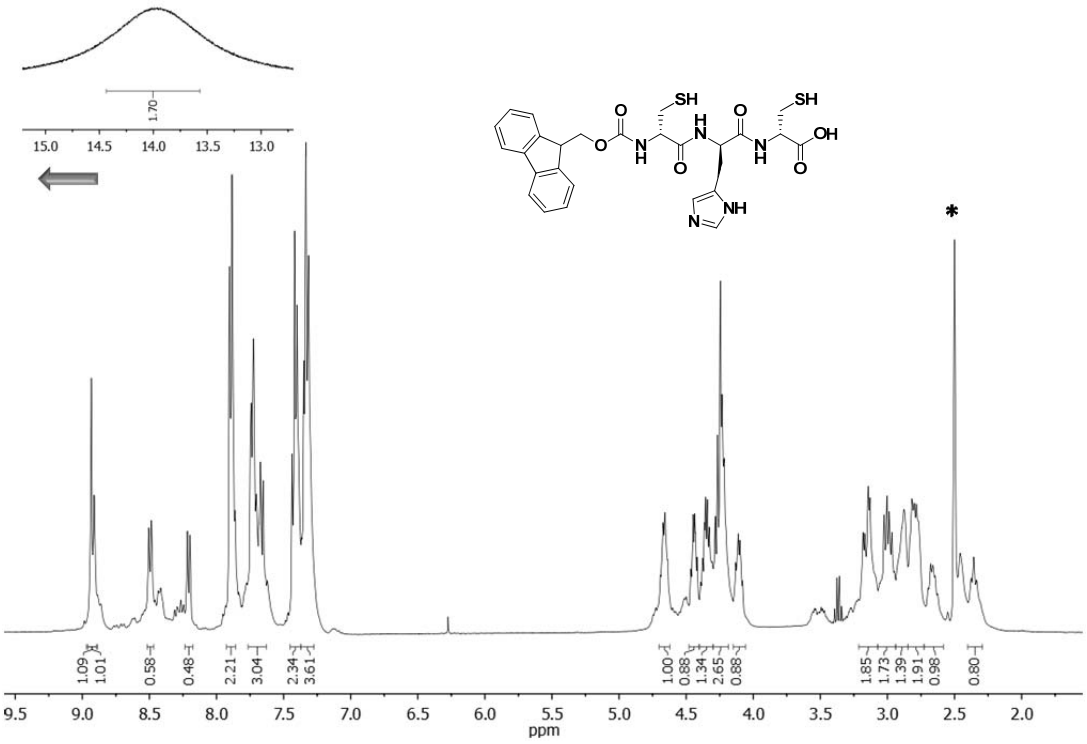

Figure S3: ^{1}H-NMR spectrum of Fmoc-L-Cys-L-His-L-Cys-OH **2** in DMSO-d_6* at 300 K.

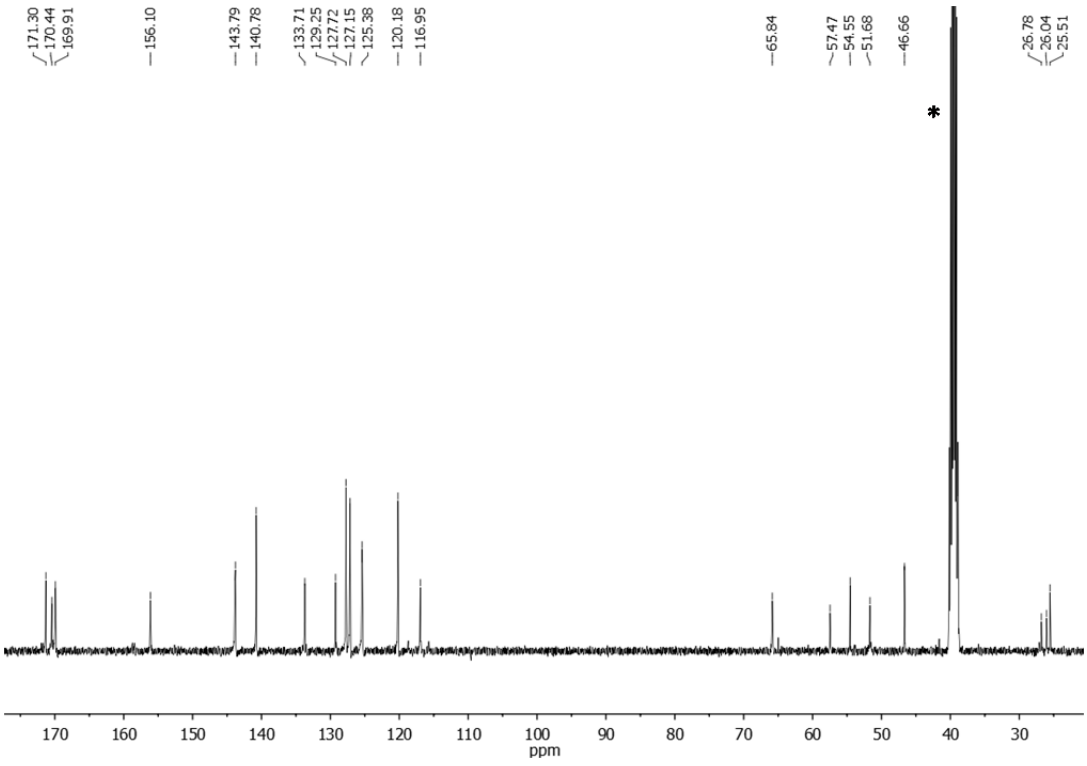

Figure S4: ^{13}C-NMR spectrum of Fmoc-L-Cys-L-His-L-Cys-OH **2** in DMSO-d_6* at 300 K.

VISUALIZATION OF PH RESPONSE OF MACROSCOPIC GELATION BEHAVIOR

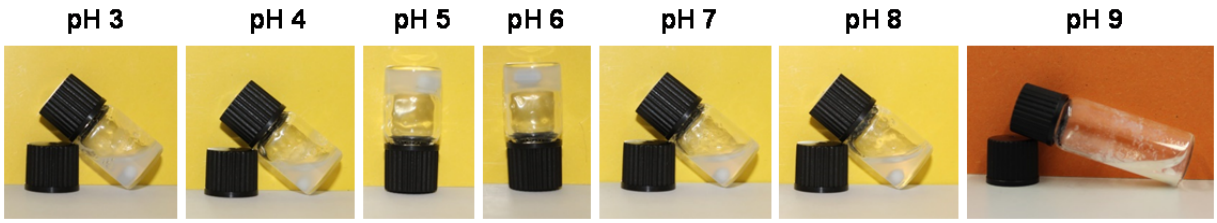

Figure S5: Pictures of 1.5 wt% **1** in water at increasing pH values. The picture of the material at pH 9 was taken with a different sample because of the irreversible degradation of gelator peptide **1**.

STEADY SHEAR RHEOLOGICAL MEASUREMENTS AT DIFFERENT PH VALUES

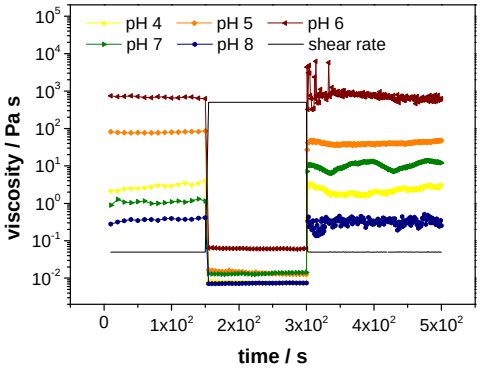

Figure S6: Step rate rheological measurements display the different recovery of the hydrogel network immediately after the breakdown due to a high magnitude shear rate of a sample with 1.5 wt% **1** at different pH values. The initial viscosities are shown in comparison in Fig. 3a.

CIRCULAR DICHROISM SPECTROSCOPY OF THE HYDROGEL

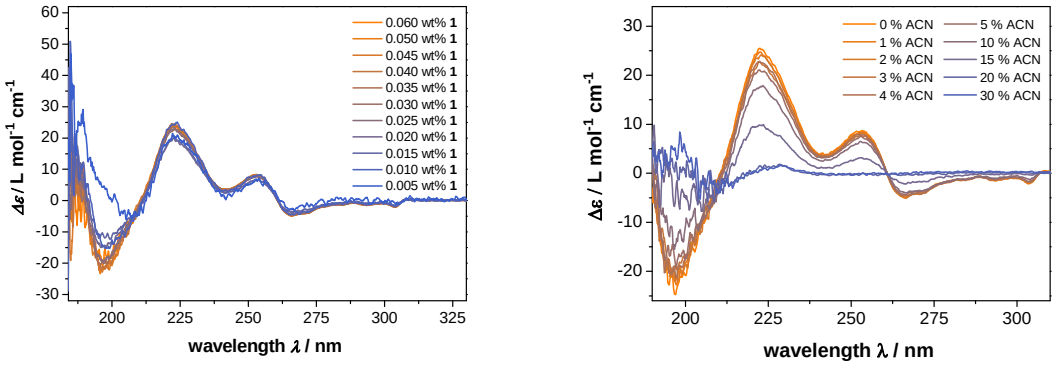

Figure S7: Circular dichroism spectrum of a diluted sample of **1** with 0.06 wt%: (*left*) Dilution of the sample with water reveals stable assemblies. (*right*) Degradation of the assemblies after addition of an organic solvent such as acetonitrile due to better solvation of monomers **1**.

SAXS DATA OF HYDROGEL AT PH 4, PH 6 AND PH 8

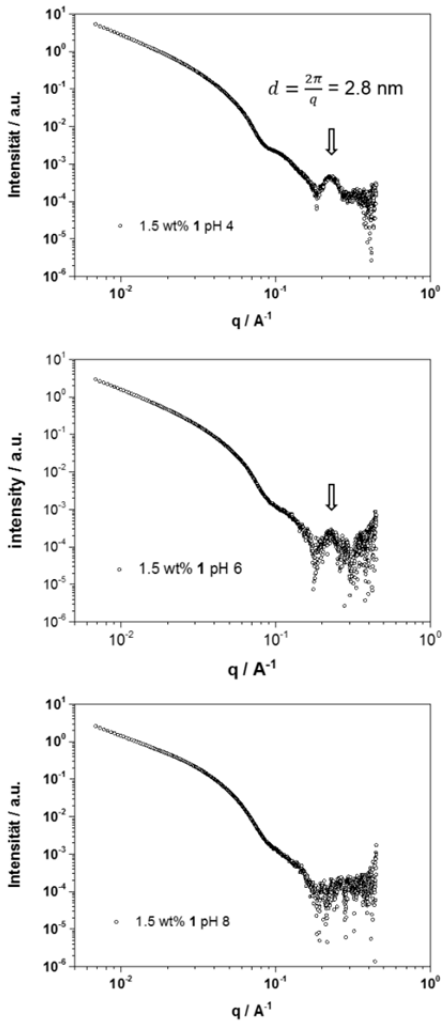

Figure S8: Small-angle X-ray scattering profile of the hydrogel with 1.5 wt% **1** at pH 4 (*top*), pH 6 (*middle*) and pH 8 (*bottom*) with strong indication for bilayers with a thickness of 2.8 nm at pH 4 and pH 6.

AGGREGATION PROPENSITY ACCORDING TO MD SIMULATION

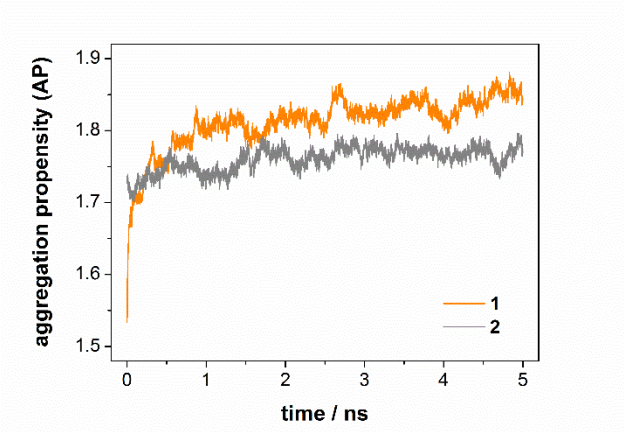

Figure S9: Evolution of the aggregation propensity of peptides **1** and **2** over the course of the MD simulation. All solvent accessible surface areas were calculated with a ball radius of 0.14 nm.

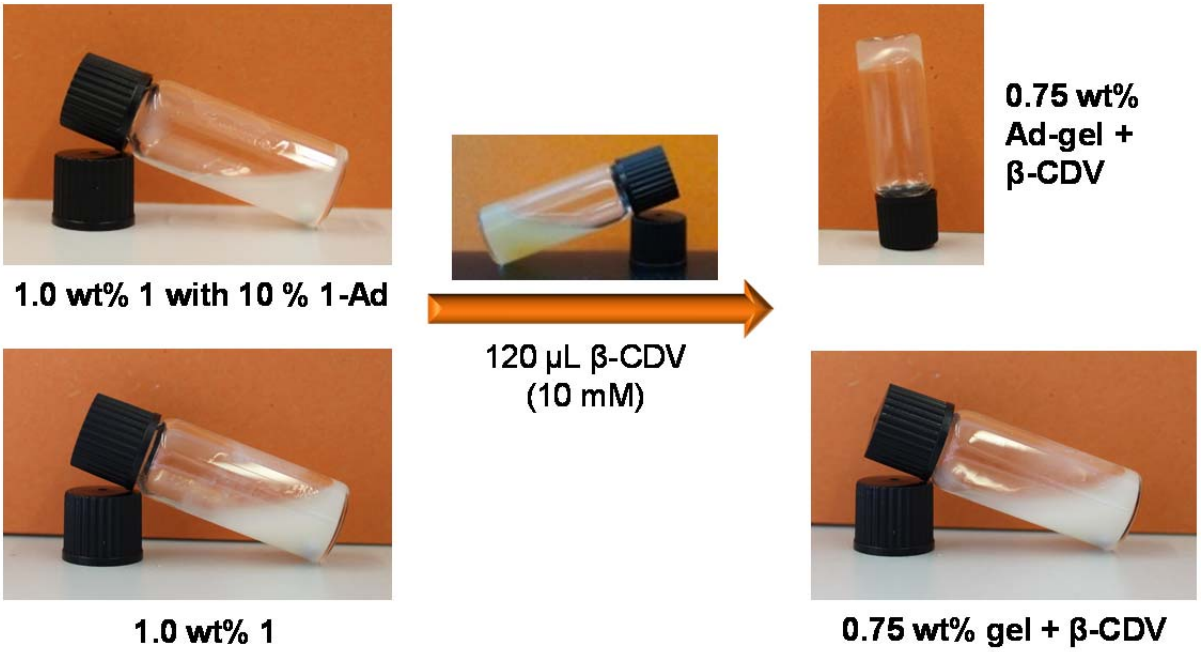

Figure S10: Control samples of the vesicle incorporation into the gel network at pH 6. (*Top*) Gel stabilization induced by cross linkage of the gel network due to molecular recognition of the adamantane functionalized monomer **1-Ad** and CDV. (*Bottom*) No interaction of the unfunctionalized hydrogel prepared from **1** with CDV. (final concentrations are 0.75 wt% of **1** with 2 mM (0.6 wt%) CDV).

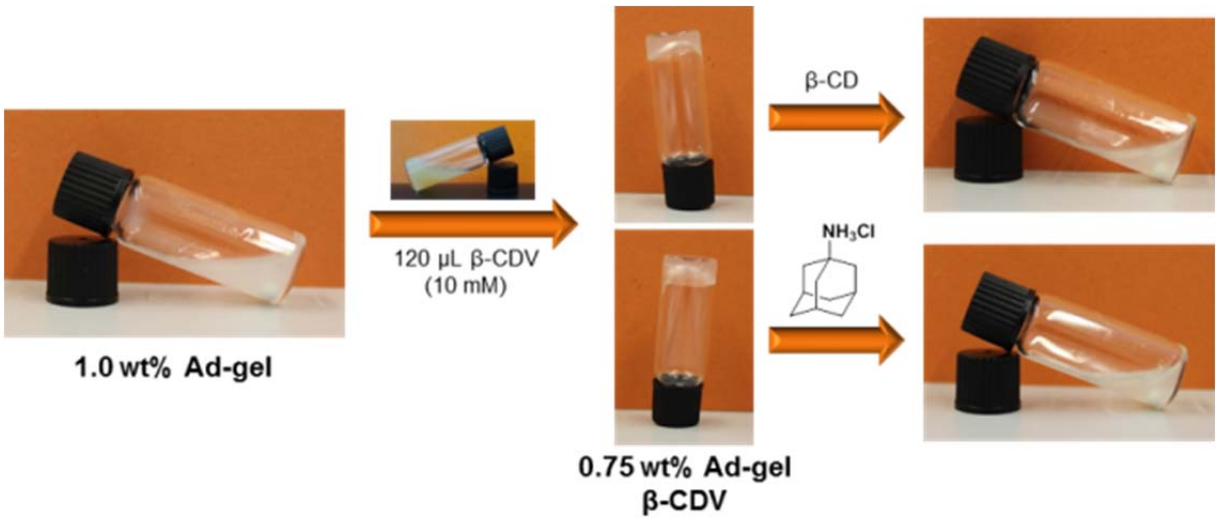

Figure S11: Responsive of supramolecular hydrogels of peptides and CDV towards competitive host and guest at pH 6. The gels were prepared from 1.0 wt% Ad-gel and addition of 120 µL CDV resulting in 0.75 wt% crosslinked hydrogel. Addition of an excess of competitive host and guest disrupts the gel network. (final concentrations are 0.75 wt% of **1** with 2 mM (0.6 wt%) CDV; β-CD and 1-adamantane ammonium chloride were added as solids to avoid dilution until effect was visible).

CHARMM PARAMETERS FOR FMOC

CHARMM atom assignments including parcial charges for Fmoc. All remaining parameter were taken from the CHARMM 35b3 parameter files when available.

```
RESI FMO         0.00
GROUP
ATOM C1   CG2R61  -0.125
ATOM H1   HGR61    0.090
ATOM C2   CG2R61  -0.085
ATOM H2   HGR61    0.085
ATOM C3   CG2R61  -0.090
ATOM H3   HGR61    0.085
ATOM C4   CG2R61  -0.130
ATOM H4   HGR61    0.085
ATOM C5   CG2R67   0.070
ATOM C6   CG2R67   0.065
ATOM C7   CG2R61  -0.130
ATOM H7   HGR61    0.085
ATOM C8   CG2R61  -0.090
ATOM H8   HGR61    0.085
ATOM C9   CG2R61  -0.085
ATOM H9   HGR61    0.085
ATOM C10  CG2R61  -0.125
ATOM H10  HGR61    0.090
ATOM C11  CG2RC0   0.060
ATOM C12  CG3C52  -0.220
ATOM H21  HGA2     0.135
ATOM C13  CG2RC0   0.060
GROUP
ATOM CF1  CG321    0.220
ATOM HF1  HGA2     0.010
ATOM HF2  HGA2     0.010
ATOM OF1  OG302   -0.360
ATOM C    CG2O1    0.800
ATOM OF2  OG2D1   -0.680
BOND C1  C2  C2  C3  C3  C4  C4  C5  C5  C6
BOND C6  C7  C7  C8  C8  C9  C9  C10 C10 C11
BOND C11 C12 C12 C13 C13 C1  C5  C13 C6  C11
BOND C1  H1  C2  H2  C3  H3  C4  H4  C7  H7
BOND C8  H8  C9  H9  C10 H10 C12 H21 C12 CF1
BOND CF1 HF1 CF1 HF2 CF1 OF1 OF1 C
DOUBLE C   OF2
BOND C   +N
```